Optica Applicata, Vol. XLII, No. 4, 2012
DOI: 10.5277/oa120417

Three-dimensional microstructures of photoresist formed by gradual gray-scale lithography approach

NINGNING LUO[1, 2*], YIQING GAO[2], ZHANG ZHIMIN[2], XIAO MENGCHAO[2], WU HUAMING[2]

[1]College of Automation Engineering, Nanjing University of Aeronautics and Astronautics, Nanjing 210016, China

[2]Key Laboratory of Nondestructive Test (Chinese Ministry of Education), Nanchang Hang Kong University, Nanchang 330063, China

[*]Corresponding author: ningningluo2002@126.com

We describe a simple and reliable approach, by employing a gradual gray-scale lithography process, which is developed for the fabrication of continuous 3D microstructure. A matrix equation has been built to quantitatively calculate the pattern gray and exposure time by combining the digital micromirror device (DMD) modulation characteristics. To avoid DMD pixel error induced by sampling, we also propose a new quantifying method in accordance with DMD pixel dimension to further improve the fabrication precision of the 3D photoresist profile. Finally, different photoresist microstructures with continuous profile, including axicon array and microlens array, have been successfully fabricated.

Keywords: gradual gray-scale lithography, DMD pixel error, axicon array, microlens array.

1. Introduction

Three-dimensional (3D) microstructures are widely used in optical and optoelectronic systems and devices [1–3], microelectromechanical systems (MEMS) and micro total analysis systems (μTAS) [4–6] due to their superior performance, compact size and easy integration. Obviously in the field of microfabrication, the ability to precisely control 3D surface profile is of great importance. At present, there are already various methods to fabricate 3D microstructures, such as reflow [7], direct writing by laser or by e-beam [8–11] and gray-scale mask [12]. In the reflow approach for photoresist pattern, it is difficult to control the surface profile accurately owning to the resist island properties (surface tension of the melted phase, resist island diameter and thickness, *etc*.) [13, 14]. Direct writing technique can overcome the drawbacks of the reflow technique by directly producing gray-scale resist masks, however, it is time consuming and expensive. As 3D microstructures become more complex, the mask cost and cycle time have increased dramatically for direct writing and gray-scale mask

techniques. As an inevitable developing trend of photolithography technology, optical maskless lithography (OML) has become more and more important in both industrial production and scientific research.

In recent years, many papers reported the SLM-based OML as well as our work [15–18]. Liquid crystal device (LCD) or digital micromirror device (DMD) serves as a dynamic mask instead of the traditional hard mask in the lithography system. LCD or DMD consists of millions of pixels and it is real-timely controlled by computer. This technique combines the flexibility of a programmable SLM-based system with the parallelism of a projection lithography system. The SLM-based area-write technique overcomes the shortcoming of lower production capacity, higher production cost and complicated process operation.

In this paper, a gradual gray-scale lithography approach is described to precisely control the surface profile. In reference [19], a similar maskless gray-scale lithography process based on DMD has been studied. The author qualitatively analyzed that the variable pattern and exposure parameters of each layer can precisely control exposure. However, our work concentrates on the quantitative calculation of gray value and exposure time according to the desired exposure dose. Combined with the DMD mod-

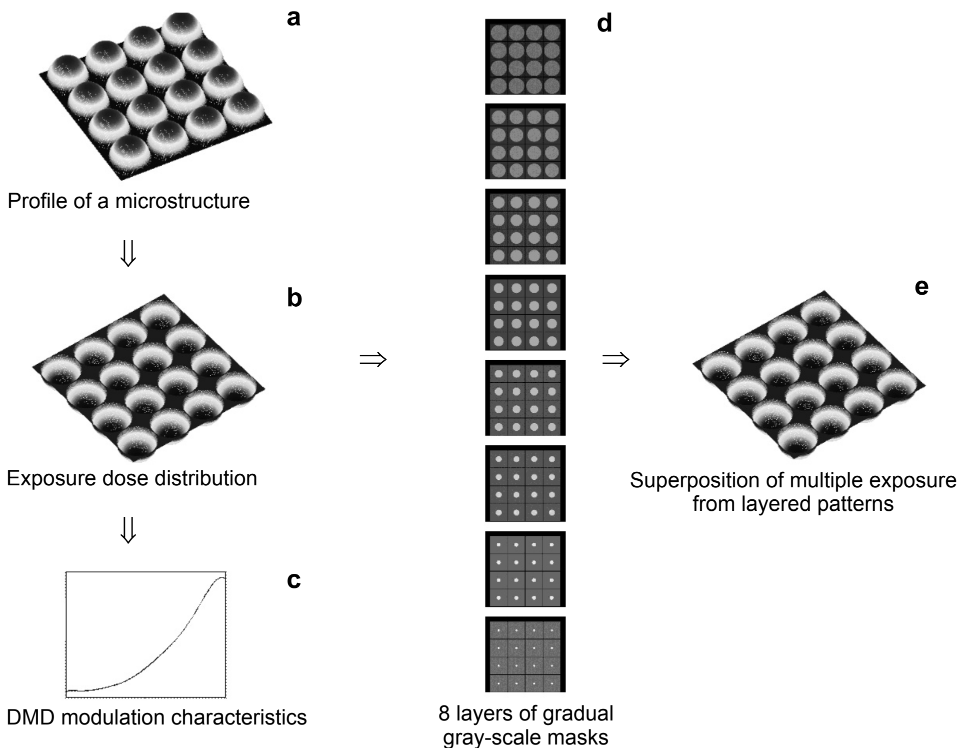

Fig. 1. Design process of 3D microstructure by using gradual gray-scale lithography.

ulation characteristics, a matrix equation has been built to precisely calculate the pattern gray and exposure time. In addition, to avoid DMD pixel error induced by sampling, we also propose a new quantifying method in accordance with DMD pixel dimension to further improve the fabrication precision of the 3D photoresist profile.

2. Principle of gradual gray-scale lithography approach

2.1. Description of the method

Figure 1 illustrates the fabrication process of a 3D microstructure by using the gradual gray-scale lithography approach. First, from the target profile (**a**), the desired exposure dose distribution (**b**) is determined. Then considering the DMD modulation characteristics (**c**), example of 8-layered gradual gray-scale masks (**d**) are derived from the exposure dose distribution. Finally, superposition of multiple exposure dose from layered patterns (**e**) is adopted to realize the microstructure profile.

In Figure 2, each layer of pattern is divided into two areas and they are filled with different gray values. For instance, each layer of pattern includes the areas in circle and outside circle and the diameter of circle accords with a changing regularity. From pattern 1 to pattern 8, the gray values and the corresponding modulated light intensity of two areas are defined in Table 1. There is an association between the gray value and

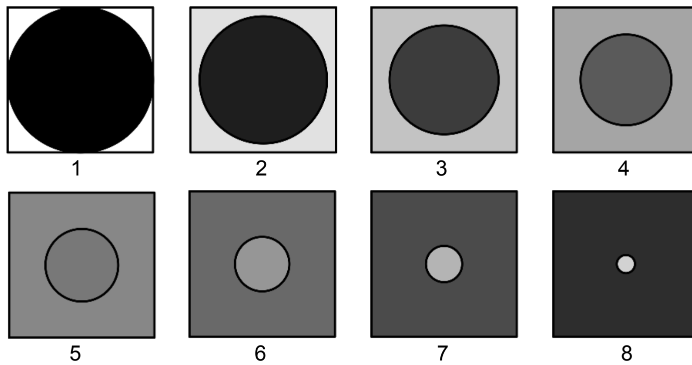

Fig. 2. Schematic diagram of the gradual gray-scale lithography.

T a b l e 1. Gray values and corresponding modulated light intensity of two areas in pattern 1–8.

Pattern number	1	2	3	4	5	6	7	8
Gray value of area in circle	a_1	a_2	a_3	a_4	a_5	a_6	a_7	a_8
Corresponding intensity	I_1	I_2	I_3	I_4	I_5	I_6	I_7	I_8
Gray value of area outside circle	b_1	b_2	b_3	b_4	b_5	b_6	b_7	b_8
Corresponding intensity	I'_1	I'_2	I'_3	I'_4	I'_5	I'_6	I'_7	I'_8
Exposure time	t_1	t_2	t_3	t_4	t_5	t_6	t_7	t_8

the modulated light intensity (see Fig. 1**c**). After the superimposed exposure of eight layers of patterns, eight areas with different exposure dose are formed. From external to internal, the exposure doses distribution of eight areas is as follows:

$$f(k) = \sum_{i=k+1}^{N} I_i' t_i + \sum_{i=1}^{k} I_i t_i, \qquad k = 1, 2, ..., N \tag{1}$$

where k represents the area number from external to internal, N is the number of layered patterns. According to Eq. (1), the desired exposure dose distribution can be obtained by appropriately choosing the gray values and the exposure time of each pattern. For simplicity, each layer of pattern is assumed to have the same exposure time. Thus, Eq. (1) becomes

$$f(k) = \left(\sum_{i=k+1}^{N} I_i' + \sum_{i=1}^{k} I_i \right) t \tag{2}$$

According to a target 3D profile, we can obtain the desired exposure dose function $E(x, y)$. Then it is quantified into N values from E_1 to E_N in a certain way. We make Eq. (2) equal to E_k ($k = 1, \ldots, N$), I_i and I_i' can be solved and the corresponding gray values can be obtained. The solving solution can be written as

$$AI + BI' = \frac{E}{t} \tag{3}$$

where: $A = \begin{bmatrix} 1 & 1 & \ldots & 1 & 1 \\ 1 & 1 & \ldots & 1 & 0 \\ \vdots & \vdots & \vdots & \vdots & \vdots \\ 1 & 1 & \ldots & 0 & 0 \\ 1 & 0 & \ldots & 0 & 0 \end{bmatrix}_{N \times N}$, $B = \begin{bmatrix} 0 & 0 & \ldots & 0 & 0 \\ 0 & 0 & \ldots & 0 & 1 \\ \vdots & \vdots & \vdots & \vdots & \vdots \\ 0 & 0 & \ldots & 1 & 1 \\ 0 & 1 & \ldots & 1 & 1 \end{bmatrix}_{N \times N}$, $I = \begin{bmatrix} I_1 \\ I_2 \\ \vdots \\ I_{N-1} \\ I_N \end{bmatrix}_{N \times 1}$,

$I' = \begin{bmatrix} I_1' \\ I_2' \\ \vdots \\ I_{N-1}' \\ I_N' \end{bmatrix}_{N \times 1}$, $E = \begin{bmatrix} E_1 \\ E_2 \\ \vdots \\ E_{N-1} \\ E_N \end{bmatrix}_{N \times 1}$.

In order to realize a liner change of exposure dose for all the exposed areas, the gray values in circles should be the same and the gray values outside circles should be the same as well for all the patterns, namely $I_1 = I_2 = ... = I_N$, $I_1' = I_2' = ... = I_N'$. If a nonlinear change of exposure dose is needed, the one is given a fixed value and

the other changes in a certain way. The above analysis indicates that the gradual gray-scale lithography approach is suitable for both linear and nonlinear surface profile. In particular, since 3D surface profile can be transformed into the exposure distribution, the quantification of exposure dose is actually the quantification of surface profile. When DMD displays the quantified size, the DMD pixel error appears due to the pixel structure, which should be considered during the mask design.

2.2. DMD pixel error

When the designed mask is sampled by DMD pixel size, the non-integer pixel error has arisen, namely the DMD pixel error. The DMD pixel error causes a deviation between the designed size and the fabricated size, which has a great influence on the quality and performance of microstructures.

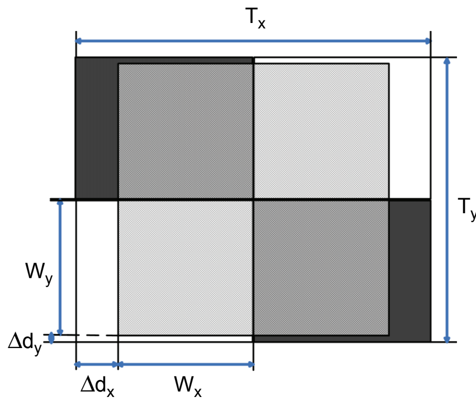

◀ Fig. 3. DMD pixel error.

Figure 3 illustrates the DMD pixel error induced by sampling. If we suppose that the mask critical dimension (CD) is $T_x \times T_y$ and the DMD pixel is $W_x \times W_y$, we can obtain Eq. (4) based on the sampling theory

$$W_x \leq \frac{T_x}{2}, \quad W_y \leq \frac{T_y}{2} \tag{4}$$

Thus, when we design the mask CD, the pixel dimensions of DMD should be considered. And the DMD pixel error can be expressed as

$$\Delta d = 2\Delta d_x \times 2\Delta d_y = \frac{\mathrm{mod}(T_x / W_x)}{\beta} \times \frac{\mathrm{mod}(T_y / W_y)}{\beta} \tag{5}$$

where β is the reduction factor of reduction lens.

In one dimension, Eq. (5) becomes

$$\Delta d_x = \frac{\mathrm{mod}(T_x / W_x)}{\beta} \tag{6}$$

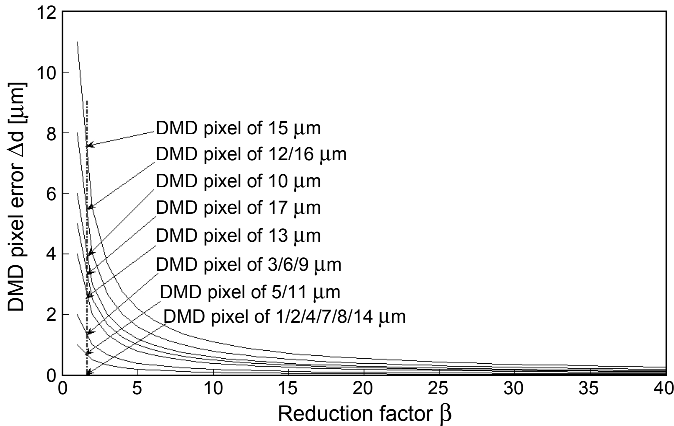

Fig. 4. Curve of DMD pixel error.

The relation between DMD pixel error and DMD pixel dimension or reduction factor β can be simulated by Eq. (6), as shown in Fig. 4. Figure 4 shows that DMD pixel error increases with the reduction factor of reduction lens. When the reduction factor is greater than 10, the variation in DMD pixel error tends towards stability. In addition, DMD pixel error also increases with the increasing of DMD pixel dimension. It is worth notice that when the mask CD is an integer multiple of DMD pixel dimension, the DMD pixel error must be zero. Consequently, the DMD pixel error can be avoided if we design the mask CD as an integer multiple of DMD pixel dimension. In the following sections, we detailedly describe the design process based on the above-mentioned rule.

2.3. Layered pattern design for various microstructures

2.3.1. Design for axicon with a linear surface profile

Axicon, with a linear surface profile, can be used to convert a parallel laser beam into a ring, to create a non-diffractive Bessel beam or to focus a parallel beam into long focus depth. During the process of profile quantification, unlike the traditional constant-height quantification, each quantitative radius is just an integer multiple of DMD pixel in order to avoid the DMD pixel error as shown in Fig. 5. The 16 isopachous layers with different diameters are adopted to approximate the linear profile. The radius variation between two adjacent layers is the same, namely $\Delta r_1 = \Delta r_2 = \ldots = \Delta r_{15}$. The desired exposure dose distribution of an axicon with diameter of 64 μm is shown in Fig. 6. Correspondingly, the exposure dose is divided into 16 isopachous layers. According to the conclusions in Section 2.1, the gray values in circles should be the same and the gray values outside circles should be the same as well for all the patterns, so there are only two variables in Eq. (3). The exposure dose is just quantified

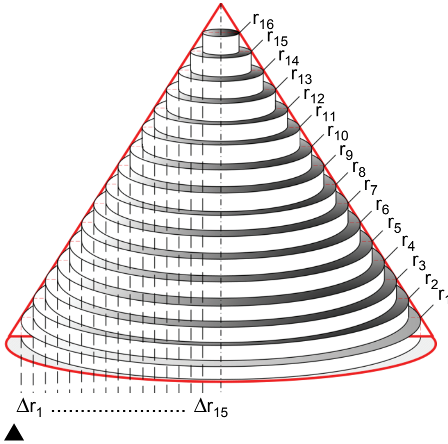

Fig. 5. Process of profile quantification.

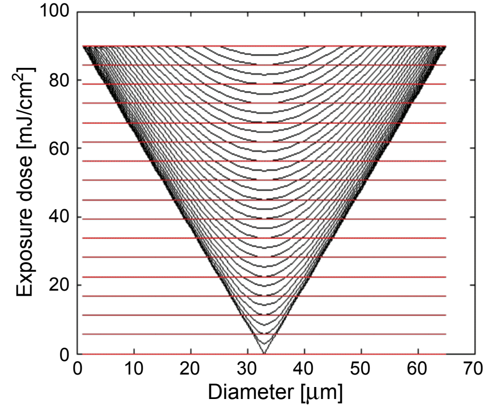

Fig. 6. Exposure dose distribution of axicon.

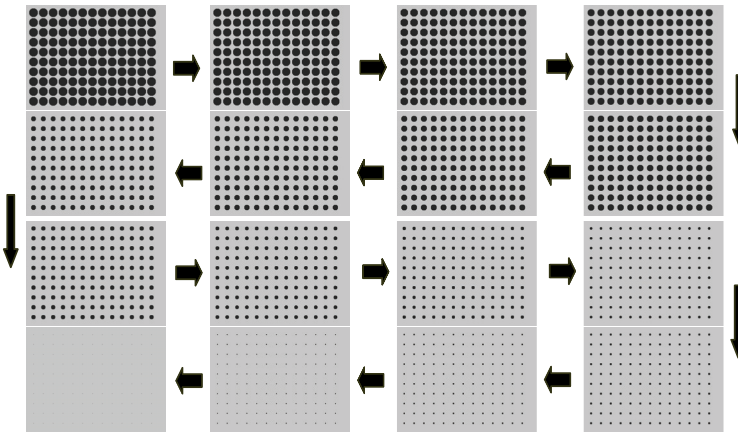

Fig. 7. The 16 layers of axicon array masks.

into two values to solve Eq. (3). The solutions of Eq. (3) are light intensities, the gray values should be calculated according to the characteristics of DMD optical modulation. To achieve approximately continuous surface profile, 16 layers of masks have been designed for the fabrication of 10×13 axicon array (given in Fig. 7).

2.3.2. Design for microlens with a nonlinear surface profile

Microlens with a nonlinear surface profile, are important integrated optical components for light focusing, array illumination, imaging, display, and optical data storage. The profile quantization of microlens is shown in Fig. 8. For microlens with a diameter of 64 μm, it is divided into 16 layers with unequal height. The height of each layer can be calculated through the corresponding radius r_h which is an integer multiple of

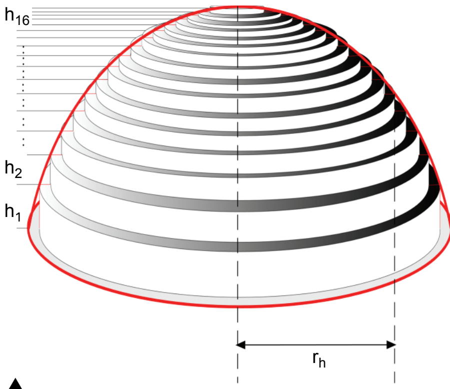

Fig. 8. Process of profile quantification.

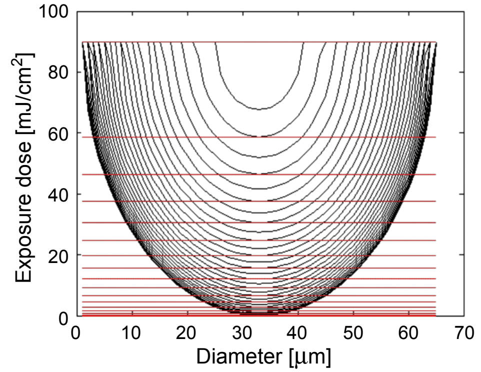

Fig. 9. Exposure dose distribution of microlens.

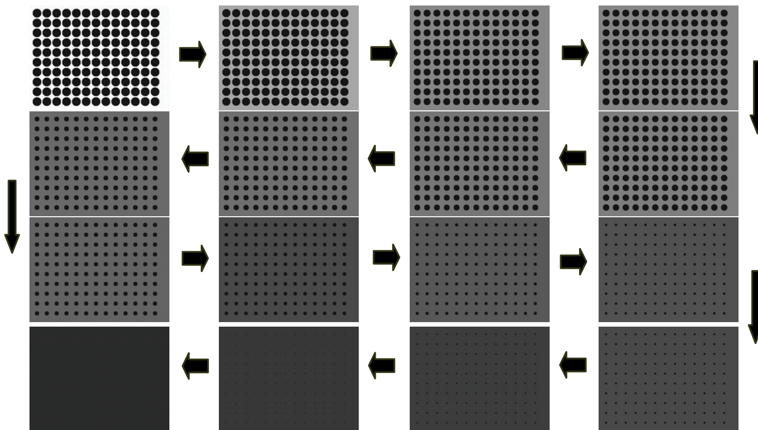

Fig. 10. The 16 layers of microlens array masks.

DMD pixel. Thus, 16-layered exposures (in Fig. 9) are used to achieve approximately continuous surface profile. $I_1 = I_2 = \ldots = I_{16}$ is assumed and Eq. (3) has sixteen variables. In order to solve the sixteen variables, the exposure dose of microlens is quantified into sixteen values from E_1 to E_{16}. In order to avoid DMD pixel error, the quantification in accordance with diameter is performed instead of the quantification according to vector height. Figure 10 shows the 16 layers of masks to be used for the fabrication of 10×13 microlens array.

3. Experiments and results

To verify the gradual gray-scale lithography method, 3D lithography experiments for an axicon array and a microlens array have been performed. Figure 11 shows the DMD-based digital lithography apparatus for 3D microfabrication developed in

our laboratory. It mostly consists of a UV source (200 W mercury lamp), a DMD chip (13.68 μm×13.68 μm), a reduction lens (14×) and a 3D translating stage. The image displayed by DMD takes place of the traditional hard mask. A photoresist coated substrate is placed on the 3D translating stage. When DMD operates, the light reflected off micromirrors is projected onto the substrate through the 14× reduction lens.

An example of the fabrication process is as follows. The positive photoresist of GP28-100 is spin-coated on a silicon substrate with a thickness of about 6 μm. Then the substrate is soft baked for 20 min at 90 °C. Following exposure, the resist is

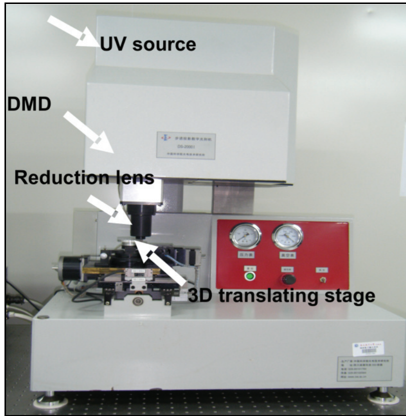

◀ Fig. 11. DMD-based digital lithography system.

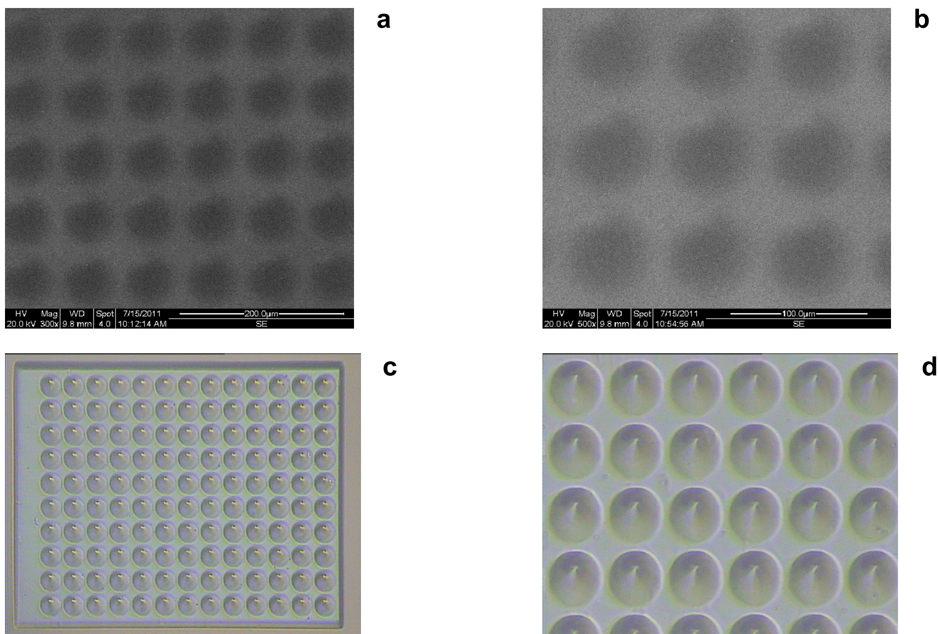

Fig. 12. Fabrication results of axicon array: SEM photograph (**a**, **b**), optical microscopy photograph (**c**, **d**).

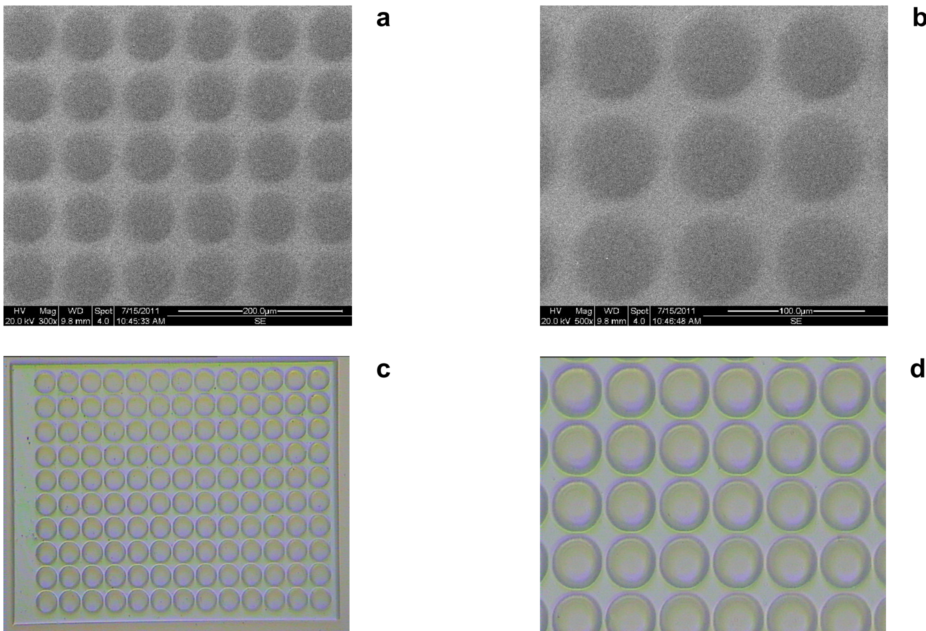

Fig. 13. Fabrication results of microlens array: SEM photograph (**a**, **b**), and optical microscopy photograph (**c**, **d**).

developed in 0.4% NaOH and 0.1% NaOH developer for 45 s and 30 s, respectively, at room temperature.

In the experiments, the layered patterns including 16 masks in Figs. 7 and 10 were exposed on the photoresist-coated silicon substrate. For the axicon, the total time for the exposure of 16 layers was about 880 s and each layer is 55 s. For the microlens, the total time was 1280 s and each mask is 80 s. Figure 12 shows the fabrication results of axicon array. Figures 12**a** and 12**b** show a scanning electron microscopy (SEM) photograph of fabricated photoresist patterns of arrayed 64 μm diameter axicon. The photographs of the axicon array measured by an optical microscope are shown in Fig. 12**c** with an enlarged portion in Fig. 12**d**. The photoresist patterns of microlens array measured by SEM and optical microscopy are shown in Fig. 13. The designed space between adjacent 64 μm diameter axicons or microlenses is 8 μm. It can be seen from Figs. 12 and 13 that the fabricated profiles are smooth and uniform. The experimental results reveal that the proposed approach is quite accurate and valid for the fabrication of continuous 3D profile.

4. Conclusions

This paper reports a simple and reliable approach for the fabrication of continuous 3D microstructure by using a gradual gray-scale lithography process. We have also built a theoretical model for the design of gradual gray-scale masks. Considering

DMD pixel error, a new quantifying method in accordance with DMD pixel dimension is presented to promote the fabrication precision. Experimental results prove that our approach of gradual gray-scale lithography can yield a smooth and uniform profile of different 3D microstructures. However, the fabricated size of microstructures is limited to the resolution of our lithography system (approximate to 1 μm) and the new quantifying method. So the fabricated diameters of axicon and microlens are more than 30 μm. Future work will be concentrated on the promotion of fabrication accuracy and the fabrication of complex aspheric and rotationally asymmetric microstructures.

Acknowledgements – This work was supported by the Chinese Nature Science Grant (60777046, and 61072131).

References

[1] REN YANG, SOPER S.A., WANJUN WANG, *Microfabrication of pre-aligned fiber bundle couplers using ultraviolet lithography of SU-8*, Sensors and Actuators A: Physical **127**(1), 2006, pp. 123–130.

[2] CAIJUN KE, XINJIAN YI, ZHIMOU XU, JIANJUN LAI, *Monolithic integration technology between microlens arrays and infrared charge coupled devices*, Optics and Laser Technology **37**(3), 2005, pp. 239–243.

[3] EITEL S., FANCEY S.J., GAUGGEL H.-P., GULDEN K.-H., BÄCHTOLD W., TAGHIZADEH M.R., *Highly uniform vertical-cavity surface-emitting lasers integrated with microlens arrays*, IEEE Photonics Technology Letters **12**(5), 2000, pp. 459–461.

[4] CHANGQING YI, CHEUK-WING LI, SHENGLIN JI, MENGSU YANG, *Microfluidics technology for manipulation and analysis of biological cells*, Analytica Chimica Acta **560**(1–2), 2006, pp. 1–23.

[5] ZHANG X., JIANG X.N., SUN C., *Micro-stereolithography of polymeric and ceramic microstructures*, Sensors and Actuators A: Physical **77**(2), 1999, pp. 149–156.

[6] CHENG SUN, XIANG ZHANG, *The influences of the material properties on ceramic micro-stereolithography*, Sensors and Actuators A: Physical **101**(3), 2002, pp. 364–370.

[7] HSIHARNG YANG, CHING-KONG CHAO, MAU-KUO WEI, CHE-PING LIN, *High fill-factor microlens array mold insert fabrication using a thermal reflow process*, Journal of Micromechanics and Microengineering **14**(8), 2004, pp. 1197–1204.

[8] CHUAN FEI GUO, SIHAI CAO, PENG JIANG, YING FANG, JIANMING ZHANG, YONGTAO FAN, YONGSHENG WANG, WENDONG XU, ZHENSHENG ZHAO, QIAN LIU, *Grayscale photomask fabricated by laser direct writing in metallic nano-films*, Optics Express **17**(22), 2009, pp. 19981–19987.

[9] CHUAN FEI GUO, JIANMING ZHANG, JUNJIE MIAO, YONGTAO FAN, QIAN LIU, *MTMO grayscale photomask*, Optics Express **18**(3), 2010, pp. 2621–2631.

[10] WANG M.R., HENG SU, *Laser direct-write gray-level mask and one-step etching for diffractive microlens fabrication*, Applied Optics **37**(32), 1998, pp. 7568–7576.

[11] TOMINAGA T., NAKAMAE K., MATSUO T., FUJIOKA H., NAKASUGI T., TAWARAYAMA K., *Electron-beam direct writing system employing character projection exposure with production dispatching rule*, Journal of Vacuum Science and Technology B **23**(6), 2005, pp. 2780–2783.

[12] REIMER K., HENKE W., QUENZER H.J., PILZ W., WAGNER B., *One-level gray-tone design – Mask data preparation and pattern transfer*, Microelectronic Engineering **30**(1–4), 1996, pp. 559–562

[13] BORRELLI N.F., *Microoptics Technology: Fabrication and Applications of Lens Arrays and Devices*, Marcel Dekker, New York, 1999, pp. 33–34.

[14] SINZINGER S., JAHNS J., *Microoptics*, Wiley-VCH, Weinheim, 1999, pp. 94–100.

[15] SUN C., FANG N., WU D.M., ZHANG X., *Projection micro-stereolithography using digital micro--mirror dynamic mask*, Sensors and Actuators A: Physical **121**(1), 2005, pp. 113–120.

[16] YI LIU, SHAOCHEN CHEN, *Direct write of microlens array using digital projection photopolymerization*, Applied Physics Letters **92**(4), 2008, article 041109.

[17] YIQING GAO, TINGZHENG SHEN, JINSONG CHEN, NINGNING LUO, XINMIN QI, QI JIN, *Research on high--quality projecting reduction lithography system based on digital mask technique*, Optik – International Journal for Light and Electron Optics **116**(7), 2005, pp. 303–310.

[18] NINGNING LUO, YIQING GAO, MIN CHEN, LIXIA YU, QING YE, *Real-time mask-division technique based on DMD digital lithography*, Optica Applicata **40**(1), 2010, pp. 239–248.

[19] KENTARO TOTSU, KENTA FUJISHIRO, SHUJI TANAKA, MASAYOSHI ESASHI, *Fabrication of three-dimensional microstructure using maskless gray-scale lithography*, Sensors and Actuators A: Physical **130–131**, 2006, pp. 387–392.

Received August 14, 2011
in revised form May 13, 2012